Supplementary Information

Synthesis of azadehydrobenzoannulenes exhibiting exceptional luminescence performance

Jinling Zhang,[a] Huabi Xie,[a] Yu Zuo,[a] Ningwen Sun,[a] Chengye Yuan,[a] Hongxing Jia,[b] Jinjin Ding,[c] Qiang Huang,[c] and Peng Xu[a]*

[a]*Department of Chemistry and Chemical Engineering, Chongqing University of Science and Technology, Chongqing 401331, China*

[b]*College of Materials Science and Engineering, National Engineering Research Center for Magnesium Alloys, Chongqing University, Chongqing 400044, China*

[c]*School of Chemistry and Chemical Engineering, Nantong University, Nantong 226019, China*

E-mail: xupeng@cqust.edu.cn (P. Xu)

Table of Contents

1. General information

Unless otherwise noted, materials obtained from commercial suppliers were used directly without further purification. All solvents for syntheses were purified by distillation. All solvents for photophysical properties measurements were spectrum pure. Air-sensitive reactions were all carried out under nitrogen atmosphere. Flash chromatography was performed on silica gel (300–400 mesh) using gradient of dichloromethane (DCM) or ethyl acetate (EA) in petroleum ether (PE) as eluent. NMR spectra were recorded on a Bruker ADVANCE III (^{1}H 400 MHz, ^{13}C 100 MHz) spectrometer. Chemical shifts were reported as the delta scale in ppm relative to $CHCl_3$ (δ = 7.26 ppm) for ^{1}H NMR and $CDCl_3$ (δ = 77.16 ppm) for ^{13}C NMR. NMR data were reported as follows: chemical shift, multiplicity (s = singlet, brs = broad singlet, d = doublet, dd = doublet of doublets, m = multiplet), coupling constant (Hz), and integration. High resolution mass spectrometry (HR MS) data were recorded on an Agilent 1290 Infinity liquid chromatograph coupled to an Agilent 6545XT accurate mass time-of-flight mass spectrometer, using atmospheric pressure electrospray ionization (ESI) or chemical ionization (APCI) techniques under positive mode (MeOH as the mobile phase, nitrogen as the carrier gas).

2. Synthetic procedures and characterization data

Synthesis of compound 5.

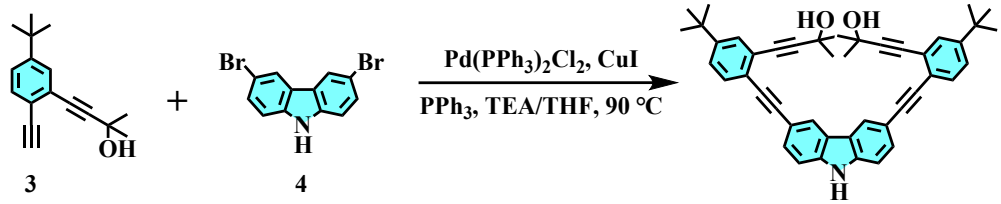

3 4 5

To a mixture of terminal alkyne **3** (5.9 g, 24.5 mmol), dibromide **4** (2.0 g, 6.2 mmol), $Pd(PPh_3)_2Cl_2$ (304.6 mg, 434 μmol), CuI (82.8 mg, 435 μmol), and PPh_3 (228.0 mg, 869 μmol) in a 150 mL Schlenk tube with a stir bar was added THF (40 mL) and triethylamine (TEA, 40 mL). Subsequently, the oxygen was removed by five consecutive freeze-pump-thaw cycles. After that, the reaction mixture was allowed to warm to room temperature and then heated to 90 °C (oil bath) with stirring for 48 hrs. After being cooled down to room temperature, the reaction solvent was removed

under vacuum. The residue was purified by flash chromatography on silica gel (PE to PE/EA = 11/1, v/v) to afford **5** (3.1 g, yield 78%) as a pale yellow foamy solid. ^{1}H NMR ($CDCl_3$, 400 MHz): δ 8.56 (s, 1H), 8.23 (s, 2H), 7.57 (dd, J = 8.4, 1.6 Hz, 2H), 7.51–7.49 (m, 4H), 7.33 (dd, J = 8.4, 2.0 Hz, 2H), 7.30 (d, J = 8.4 Hz, 2H), 2.54 (brs, 2H), 1.71 (s, 12H), 1.33 (s, 18H). ^{13}C NMR ($CDCl_3$, 100 MHz): δ 151.0, 139.6, 131.5, 130.0, 129.0, 125.6, 124.7, 124.1, 123.6, 123.0, 114.6, 111.1, 97.3, 94.0, 86.9, 81.9, 66.1, 34.8, 31.8, 31.2. FT-IR (KBr): ν_{max} 3416, 3196, 2965, 2868, 2815, 2205, 1632, 1608, 1497, 1393, 1378, 1352, 1279, 1241, 1161, 1123, 930 cm^{-1}. HR-MS (ESI) m/z: Calcd for $C_{46}H_{42}N$ $[M + H - 2H_2O]^+$: 608.3312, Found: 608.3341.

Synthesis of compound 6.

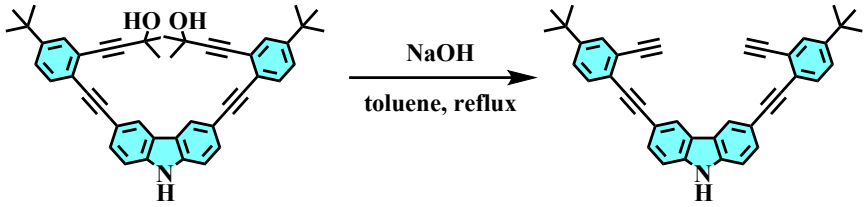

5 **6**

To a solution of diol **5** (2.7 g, 4.2 mmol) in toluene (70 mL) in a 150 mL Kjeldahl flask was added NaOH (120 mg, 3.0 mmol). Remove of the oxygen by five consecutive freeze-pump-thaw cycles. Subsequently, the reaction mixture was heated to vigorously reflux (oil bath) and stirred for 8 hrs. After being cooled down to room temperature, the reaction mixture was then placed in an ice bath and quenched by the addition of hydrochloric acid (6.0 M, 5 mL, 30.0 mmol) in one portion. The organic layer was removed, and the aqueous layer was extracted with EA. The combined organic layers were concentrated in vacuum. The residue was purified by flash chromatography on silica gel (PE to PE/DCM = 5/3, v/v) to afford **6** (1.7 g, yield 77%) as a pale yellow solid. ^{1}H NMR ($CDCl_3$, 400 MHz): δ 8.28 (s, 2H), 8.18 (s, 1H), 7.63–7.60 (m, 4H), 7.53 (d, J = 8.0 Hz, 2H), 7.39 (dd, J = 8.4, 2.0 Hz, 2H), 7.30 (d, J = 8.4 Hz, 2H), 3.43 (s, 2H), 1.34 (s, 18H). ^{13}C NMR ($CDCl_3$, 100 MHz): δ 151.1, 139.6, 131.6, 130.2, 129.7, 126.1, 124.3, 124.1, 124.0, 123.0, 114.7, 111.0, 94.2, 86.7, 83.2, 80.5, 34.8, 31.2. FT-IR (KBr): ν_{max} 3403, 3286, 3275, 2960, 2901, 2864, 2813, 2207, 1630, 1606, 1497, 1395, 1350, 1283, 1234, 1131, 1121, 881, 821 cm^{-1}. HR-MS

(ESI) m/z: Calcd for $C_{40}H_{33}N$ $[M]^+$: 527.2608, Found: 527.2624; Calcd for $C_{41}H_{38}NO$ $[M + CH_3OH + H]^+$: 560.2948, Found: 560.2930.

Synthesis of compounds azaDBAa and azaDBAb.

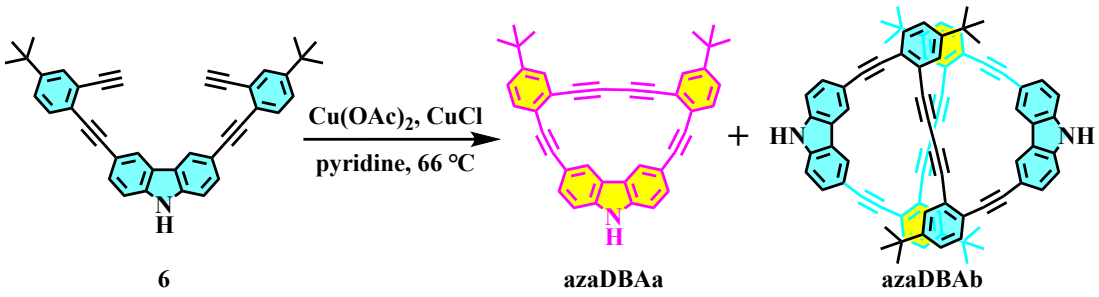

6 **azaDBAa** **azaDBAb**

To a stirred suspension of $Cu(OAc)_2$ (1.0 g, 5.5 mmol) and CuCl (545.0 mg, 5.5 mmol) in pyridine (1.2 L) open to air and heated at 66 ºC was added a solution of terminal alkyne **6** (791 mg, 1.5 mmol) in pyridine (240 mL) via syringe pump over 16 days. As the reaction was ongoing, a copy of catalyst mixture ($Cu(OAc)_2$ (1.0 g, 5.5 mmol) and CuCl (545.0 mg, 5.5 mmol)) was added to the reaction mixture every 48 hrs. After the substrate alkyne was consumed, the solvent was recovered in vacuum. Followed by the addition of DCM (120 mL) to the resulting slurry, hydrochloric acid (4.0 M) was then added until those solid dissolved completely. The organic phase was separated, and the aqueous phase was extracted with DCM. The combined organic layers were dried over anhydrous Na_2SO_4, filtered, and concentrated. The residue was purified by flash chromatography on silica gel (PE to PE/DCM) to afford **azaDBAa** (PE/DCM = 2/1, v/v) as a brown foamy solid (496 mg, yield 63%) and **azaDBAb** (PE/DCM = 2/3, v/v) as a light khaki solid (40 mg, yield 5%). Structural data for **azaDBAa**: ^{1}H NMR ($CDCl_3$, 400 MHz): δ 8.39 (s, 2H), 8.15 (s, 1H), 7.93 (s, 2H), 7.43–7.40 (m, 6H), 7.30 (d, J = 8.0 Hz, 2H), 1.40 (s, 18H). ^{13}C NMR ($CDCl_3$, 100 MHz): δ 150.7, 139.3, 134.0, 131.4, 129.7, 126.5, 125.4, 125.0, 123.2, 121.8, 115.0, 110.6, 97.1, 93.1, 85.1, 78.3, 35.0, 31.3. FT-IR (KBr): ν_{max} 3420, 2961, 2925, 2855, 2815, 2192, 1628, 1606, 1494, 1475, 1396, 1347, 1279, 1254, 1224, 1114, 893, 827, 806 cm^{-1}. HR-MS (ESI) m/z: Calcd for $C_{40}H_{32}N$ $[M + H]^+$: 526.2530, Found: 526.2545; Calcd for $C_{41}H_{35}NO$ $[M + CH_3OH]^+$: 557.2714, Found: 557.2738.

Structural data for **azaDBAb**: ^{1}H NMR ($CDCl_3$, 400 MHz): δ 7.70 (s, 4H), 7.69 (d, *J* = 2.0 Hz, 4H), 7.52–7.48 (m, 8H), 7.43 (s, 2H), 7.40 (dd, *J* = 8.4, 2.0 Hz, 4H), 6.85 (d, *J* = 8.4 Hz, 4H), 1.39 (s, 36H). ^{13}C NMR ($CDCl_3$, 100 MHz): *δ* 150.4, 138.7, 131.2, 130.2, 129.9, 126.2, 125.1, 124.2, 124.1, 122.2, 114.0, 110.1, 95.8, 86.8, 82.2, 77.8, 34.7, 31.1. FT-IR (KBr): ν_{max} 3442, 2956, 2925, 2827, 2208, 1600, 1501, 1365, 1285, 1228, 814, 772 cm^{-1}. HR-MS (APCI) m/z: Calcd for $C_{00}H_{63}N_2$ $[M + H]^+$: 1051.4986, Found: 1051.5006.

Synthesis of compound 9.

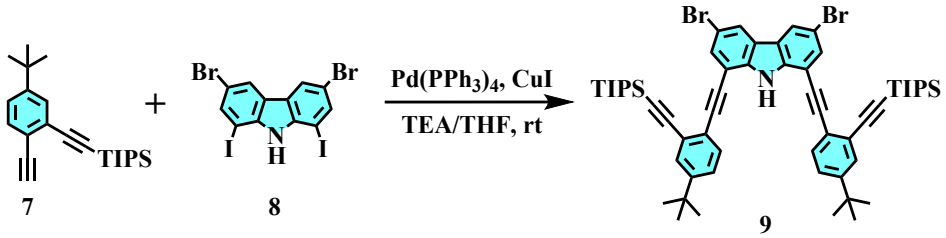

7 8 9

To a 150 mL Schlenk tube with a stir bar was added terminal alkyne **7** (3.5 g, 10.3 mmol), diiodide **8** (2.0 g, 3.5 mmol), $Pd(PPh_3)_4$ (200 mg, 173 μmol), CuI (33 mg, 173 μmol), THF (35 mL), and Et_3N (35 mL), successively. After removal of the oxygen by five consecutive freeze-pump-thaw cycles, the reaction mixture was allowed to warm to room temperature and stirred for 36 hrs. Then the reaction was quenched by addition of water and extracted with EA. The combined organic layers were washed with an aqueous solution of sodium chloride (saturated), dried over anhydrous Na_2SO_4, filtered, and concentrated in vacuum. The residue was purified by flash chromatography on silica gel (PE) to give **9** (3.0 g, yield 87%) as a pale yellow foamy solid. ^{1}H NMR ($CDCl_3$, 400 MHz): δ 8.78 (s, 1H), 8.10 (d, *J* = 2.0 Hz, 2H), 7.74 (d, *J* = 1.6 Hz, 2H), 7.57–7.54 (m, 4H), 7.34 (dd, *J* = 8.0, 2.0 Hz, 2H), 1.36 (s, 18H), 1.08–1.07 (m, 42H). ^{13}C NMR ($CDCl_3$, 100 MHz): δ 152.2, 139.0, 132.22, 132.19, 129.7, 126.1, 125.7, 123.83, 123.77, 122.4, 112.4, 108.4, 105.6, 95.3, 94.8, 86.5, 34.9, 31.2, 18.8, 11.5. FT-IR (KBr): ν_{max} 3458, 2961, 2940, 2861, 2811, 2154, 1628, 1492, 1472, 1396, 1349, 1273, 1128, 1071, 924, 880, 857 cm^{-1}. HR-MS (APCI) m/z: Calcd for $C_{58}H_{72}{}^{79}Br_2NSi_2$ $[M + H]^+$: 996.3565, Found: 996.3516; Calcd for $C_{58}H_{72}{}^{79}Br^{81}Br$

NSi_2 $[M + H]^+$: 998.3545, Found: 998.3498; Calcd for $C_{58}H_{72}{}^{81}Br_2NSi_2$ $[M + H]^+$: 1000.3524, Found: 1000.3501.

Synthesis of compound 10.

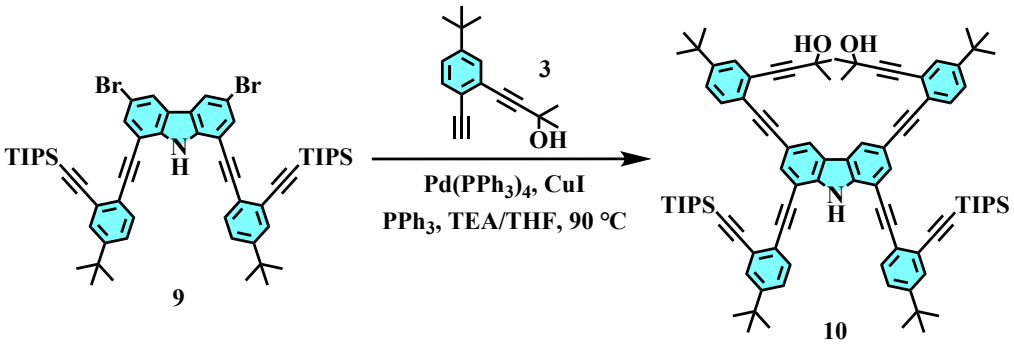

The same procedure for **5** was applied for the preparation of **10**. Flash chromatography (PE to PE/DCM = 2/5, v/v) afforded **10** (2.5 g, yield 76% from **9** (2.5 g, 2.5 mmol)) as a yellow foamy solid. ^{1}H NMR ($CDCl_3$, 400 MHz): δ 8.87 (s, 1H), 8.27 (d, J = 1.2 Hz, 2H), 7.83 (d, J = 1.6 Hz, 2H), 7.57–7.55 (m, 4H), 7.52–7.49 (m, 4H), 7.36 (dd, J = 4.4, 2.0 Hz, 2H), 7.34 (dd, J = 4.8, 2.0 Hz, 2H), 2.41 (brs, 2H), 1.73 (s, 12H), 1.35 (s, 18H), 1.34 (s, 18H), 1.063 (s, 36H), 1.055 (s, 6H). ^{13}C NMR ($CDCl_3$, 100 MHz): δ 152.0, 151.2, 140.0, 133.1, 132.2, 131.6, 129.7, 129.1, 126.0, 125.7, 125.6, 124.8, 124.6, 123.5, 123.2, 122.7, 115.5, 107.1, 105.7, 97.4, 95.1, 93.9, 92.9, 87.1, 81.7, 66.0, 34.92, 34.90, 31.9, 31.2, 18.8, 11.5. FT-IR (KBr): ν_{max} 3454, 2963, 2862, 2205, 2152, 1630, 1494, 1460, 1396, 1351, 1271, 1165, 1126, 920, 882, 827 cm^{-1}. HR-MS (ESI) m/z: Calcd for $C_{93}H_{113}NO_3Si_2$ $[M + CH_3OH]^+$: 1348.8288, Found: 1348.8351.

Synthesis of compound 11.

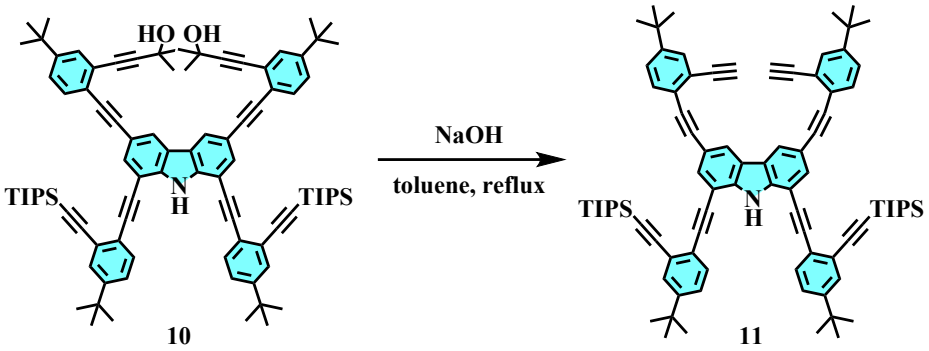

The same procedure for **6** was applied for the preparation of **11**. Flash

chromatography (PE to PE/DCM = 5/1, v/v) afforded **11** (1.3 g, yield 71% from **10** (2.0 g, 1.5 mmol)) as a brown foamy solid. ^{1}H NMR ($CDCl_3$, 400 MHz): δ 8.92 (s, 1H), 8.27 (s, 2H), 7.85 (s, 2H), 7.60–7.51 (m, 8H), 7.40 (dd, J = 8.4, 2.0 Hz, 2H), 7.34 (dd, J = 8.4, 2.0 Hz, 2H), 3.41 (s, 2H), 1.351 (s, 18H), 1.348 (s, 18H), 1.07 (m, 42H). ^{13}C NMR ($CDCl_3$, 100 MHz): δ 152.0, 151.2, 140.1, 133.2, 132.3, 131.7, 129.8, 129.7, 126.1, 126.0, 125.7, 124.7, 124.2, 123.8, 123.1, 122.7, 115.4, 107.1, 105.7, 95.2, 93.9, 93.2, 87.1, 86.9, 83.1, 80.6, 34.93, 34.89, 31.2, 18.8, 11.5. FT-IR (KBr): ν_{max} 3452, 3291, 2964, 2864, 2811, 2150, 1630, 1492, 1460, 1396, 1349, 1266, 1128, 920, 880, 827 cm^{-1}. HR-MS (ESI) m/z: Calcd for $C_{86}H_{98}NSi_2$ $[M + H]^+$: 1200.7233, Found: 1200.7182; Calcd for $C_{87}H_{101}NOSi_2$ $[M + CH_3OH]^+$: 1231.7417, Found: 1231.7446; Calcd for $C_{87}H_{102}NOSi_2$ $[M + H + CH_3OH]^+$: 1232.7495, Found: 1232.7520.

Synthesis of compound azaDBAc.

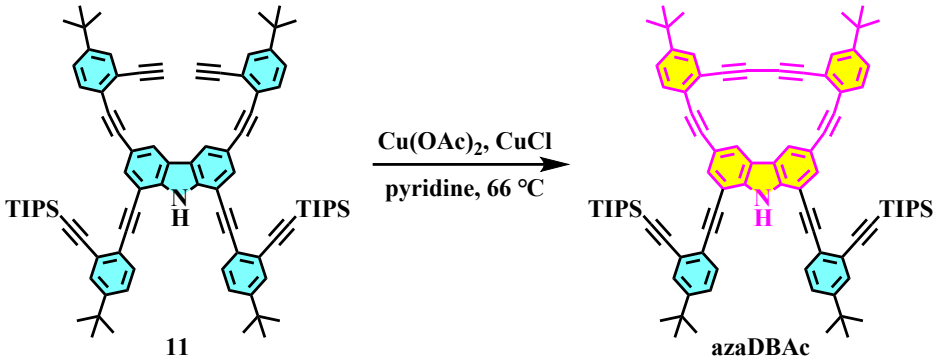

The same procedure for **azaDBAa** was applied for the preparation of **azaDBAc**. Flash chromatography (PE to PE/DCM = 5/1, v/v) afforded **azaDBAc** (455 mg, yield 76% from **11** (600 mg, 500 μmol)) as a yellow foamy solid. ^{1}H NMR ($CDCl_3$, 400 MHz): δ 8.83 (s, 1H), 8.49 (d, J = 1.2 Hz, 2H), 7.94 (s, 2H), 7.65 (d, J = 1.6 Hz, 2H), 7.59–7.55 (m, 5H), 7.45 (m, 3H), 7.36 (dd, J = 8.4, 2.0 Hz, 2H), 1.41 (s, 18H), 1.35 (s, 18H), 1.05 (m, 42H). ^{13}C NMR ($CDCl_3$, 100 MHz): δ 151.9, 151.0, 139.7, 134.1, 132.2, 131.7, 129.9, 129.7, 128.6, 126.6, 126.1, 125.7, 125.5, 123.2, 122.9, 121.6, 115.8, 106.8, 105.8, 96.2, 95.1, 93.6, 93.1, 87.8, 85.1, 78.4, 35.1, 34.9, 31.3, 31.2, 18.8, 11.5. FT-IR (KBr): ν_{max} 3455, 2961, 2925, 2861, 2827, 2154, 1608, 1492, 1463, 1363, 1260, 882, 831, 776 cm^{-1}. HR-MS (ESI) m/z: Calcd for $C_{86}H_{99}NSi_2$ $[M + NH_4]^+$: 1215.7342, Found: 1215.7365.

3. HR-MS spectra

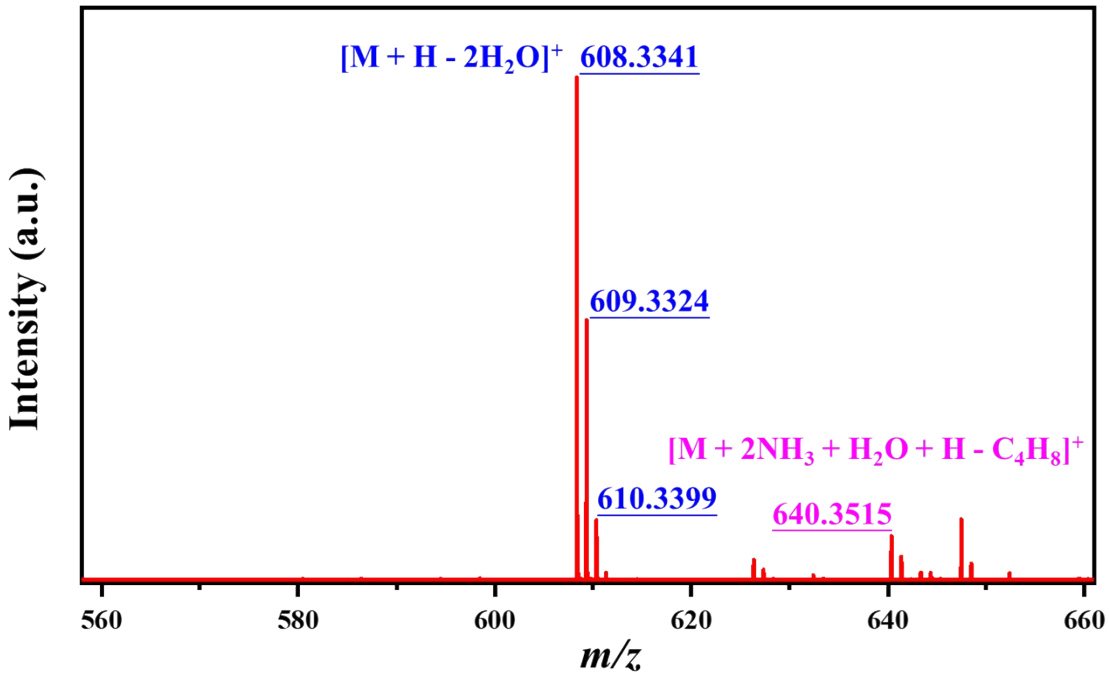

Fig. S1 HR ESI mass spectrum and isotopic distribution pattern of **5**.

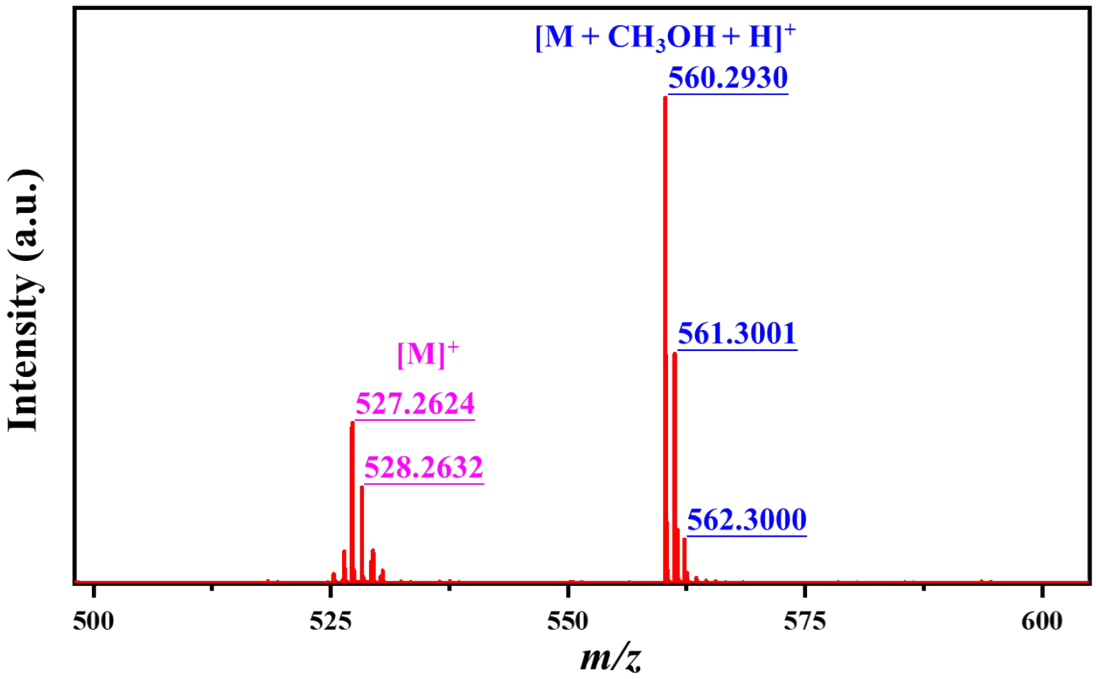

Fig. S2 HR ESI mass spectrum and isotopic distribution pattern of **6**.

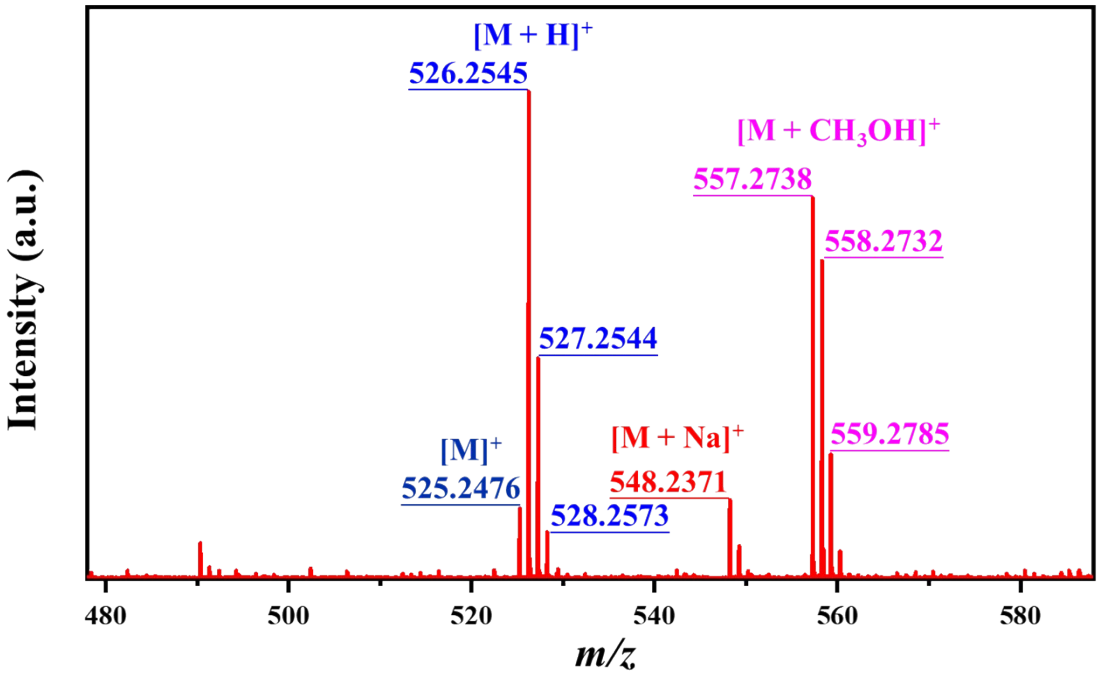

Fig. S3 HR ESI mass spectrum and isotopic distribution pattern of **azaDBAa**.

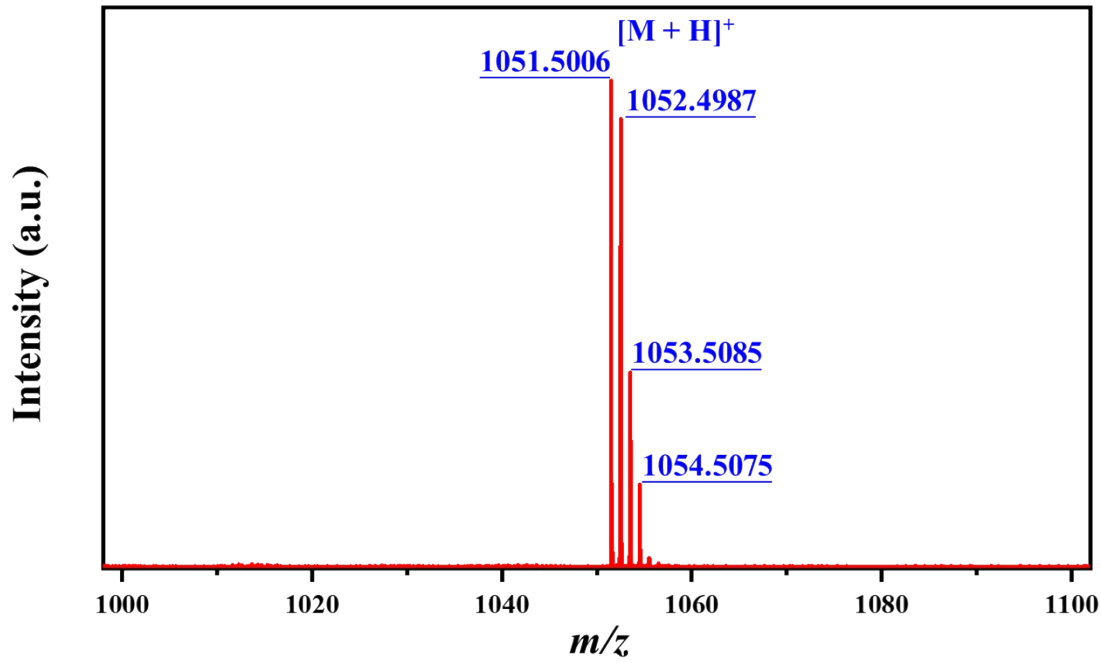

Fig. S4 HR APCI mass spectrum and isotopic distribution pattern of **azaDBAb**.

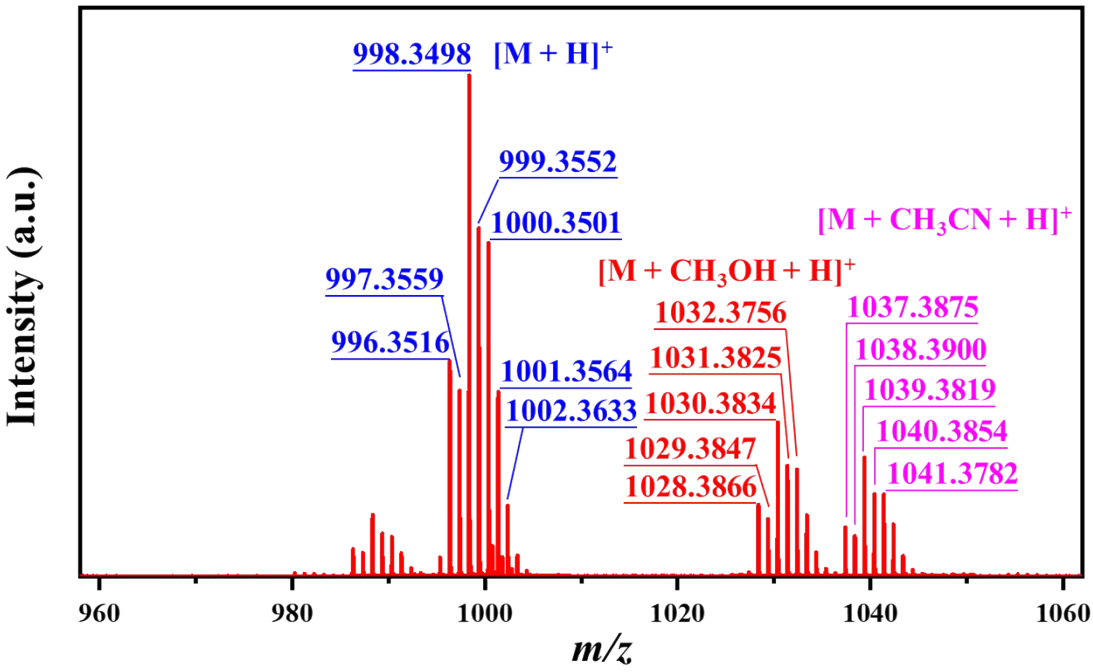

Fig. S5 HR APCI mass spectrum and isotopic distribution pattern of **9**.

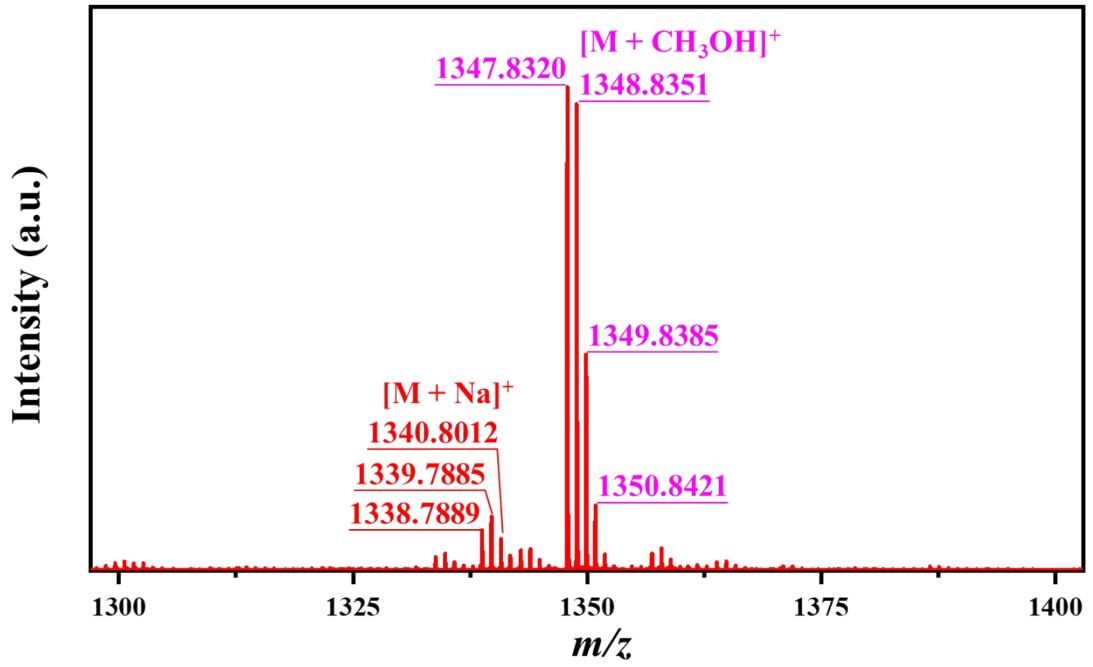

Fig. S6 HR ESI mass spectrum and isotopic distribution pattern of **10**.

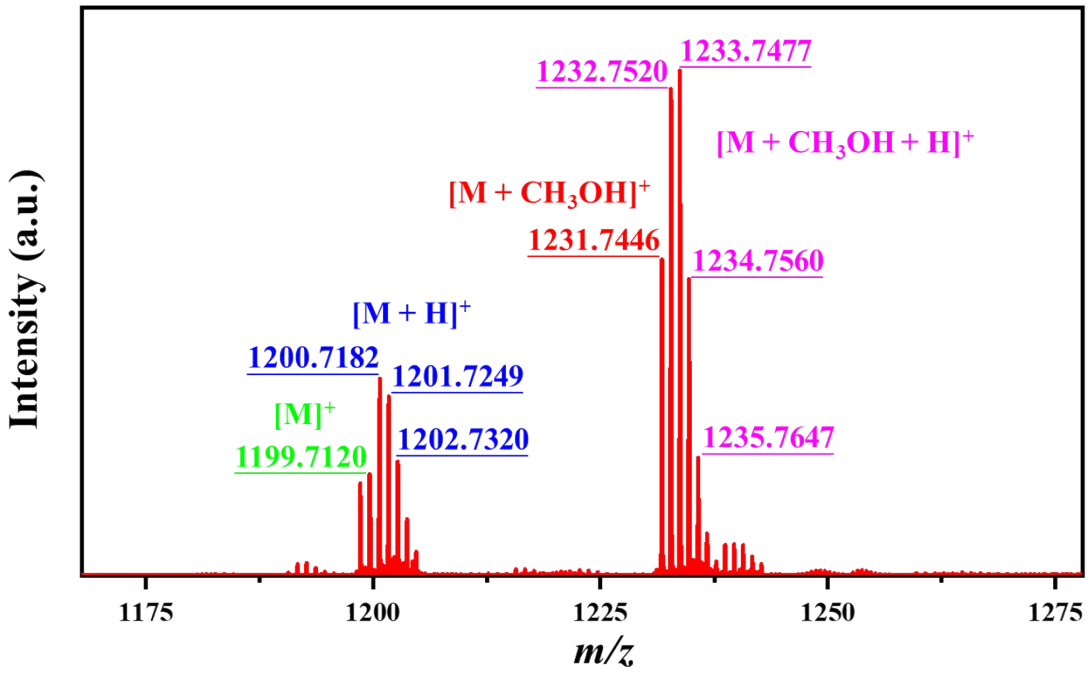

Fig. S7 HR ESI mass spectrum and isotopic distribution pattern of **11**.

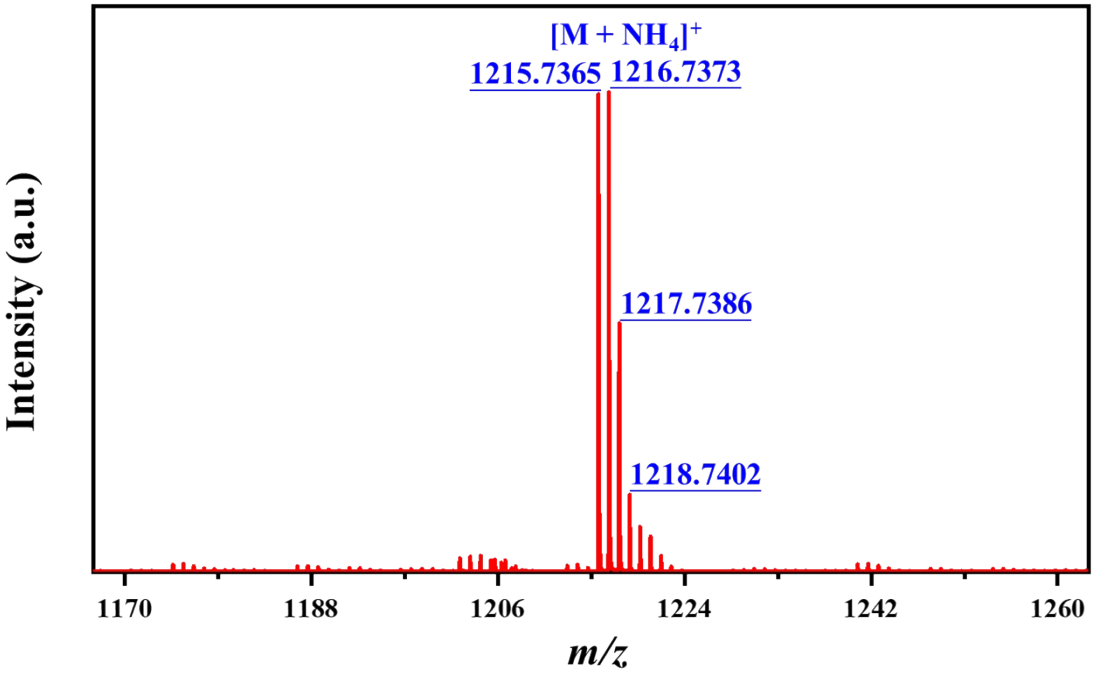

Fig. S8 HR APCI mass spectrum and isotopic distribution pattern of **azaDBAc**.

4. ^{1}H and ^{13}C NMR spectra

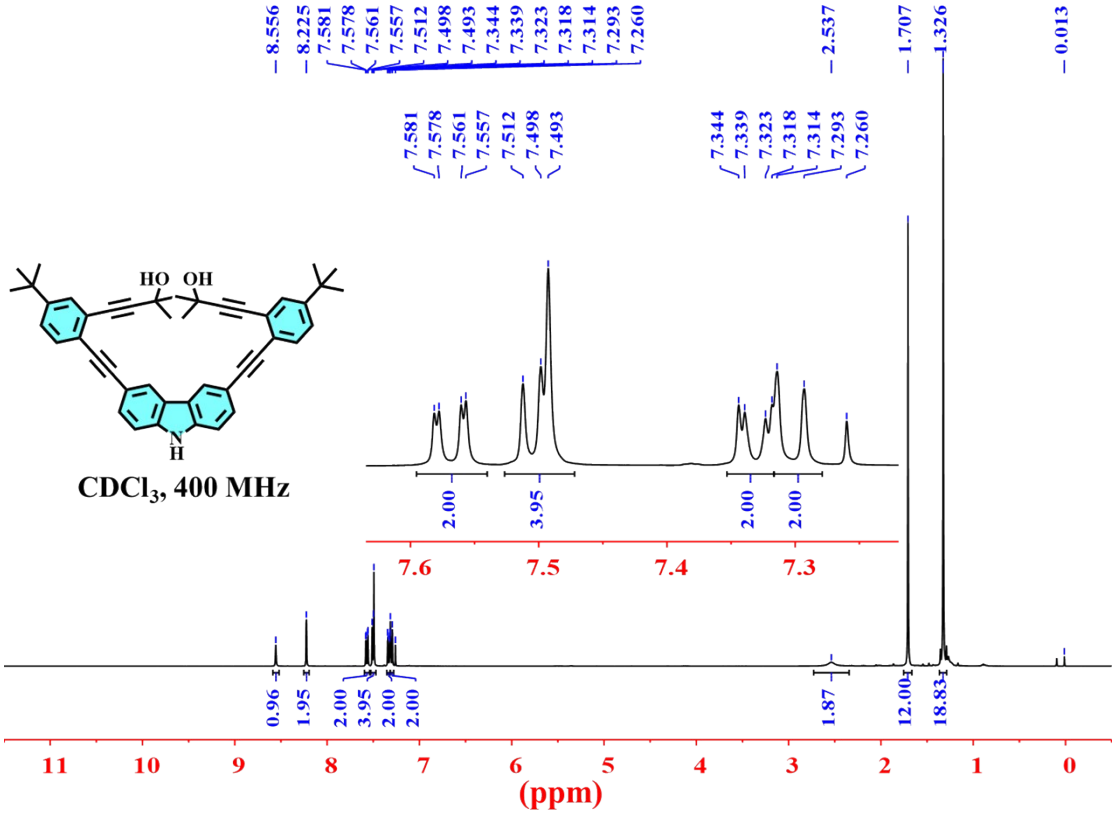

Fig. S9 ^{1}H NMR spectrum of compound **5**.

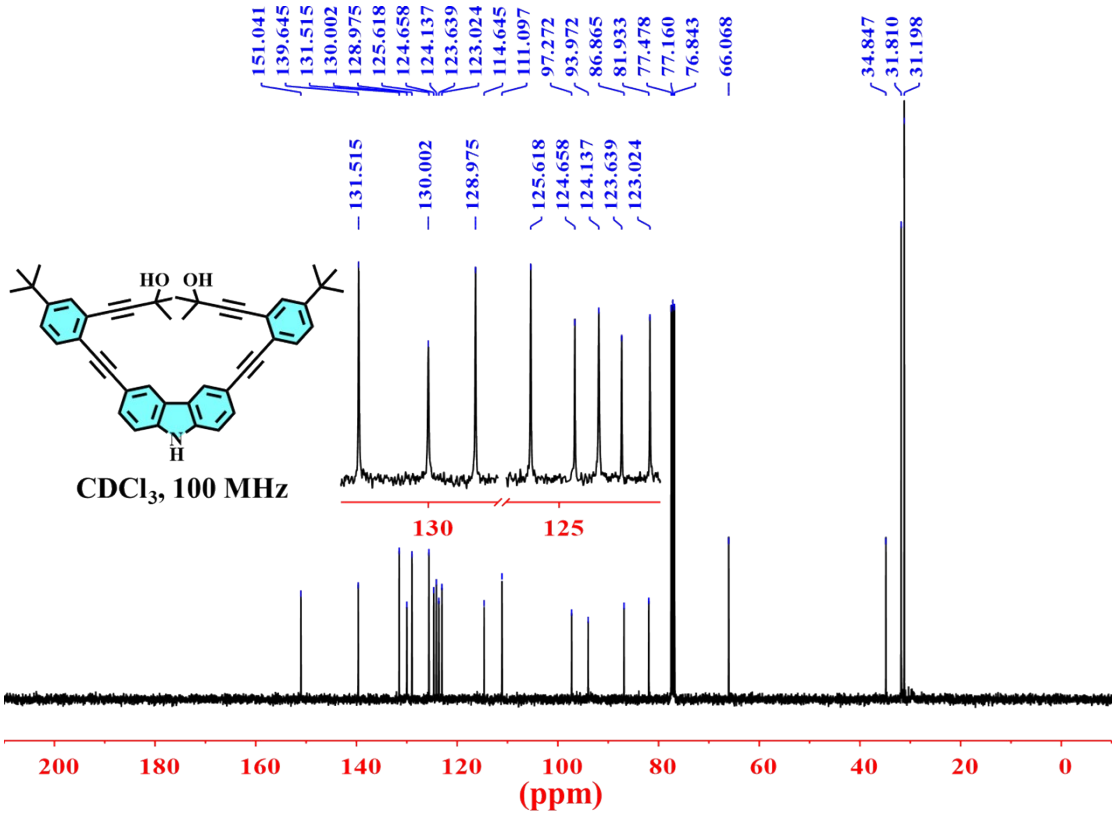

Fig. S10 ^{13}C NMR spectrum of compound **5**.

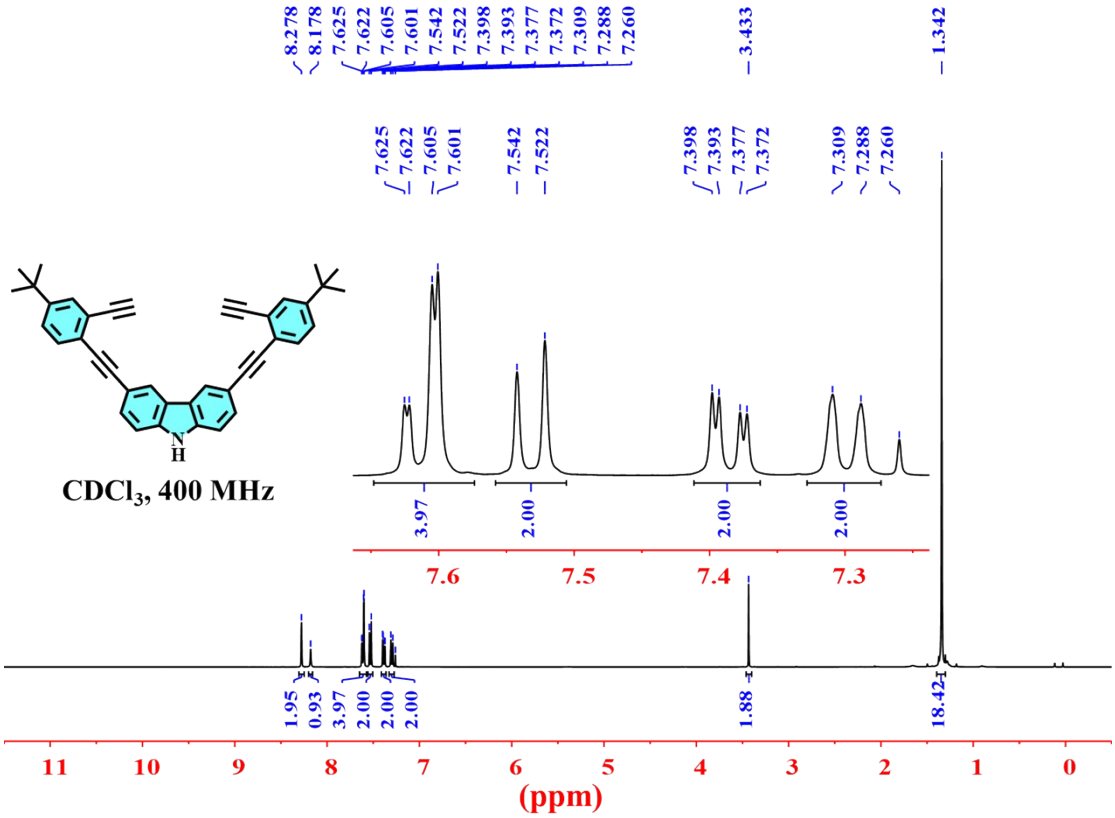

Fig. S11 ^{1}H NMR spectrum of compound **6**.

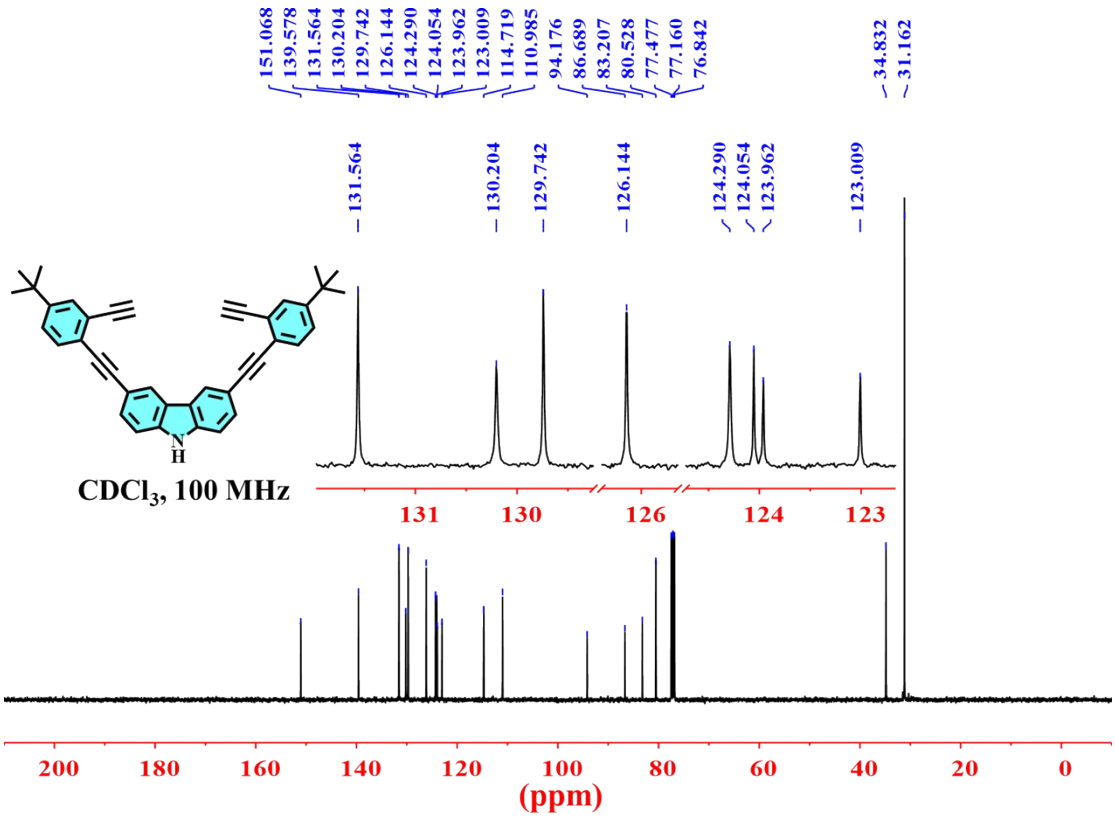

Fig. S12 ^{13}C NMR spectrum of compound **6**.

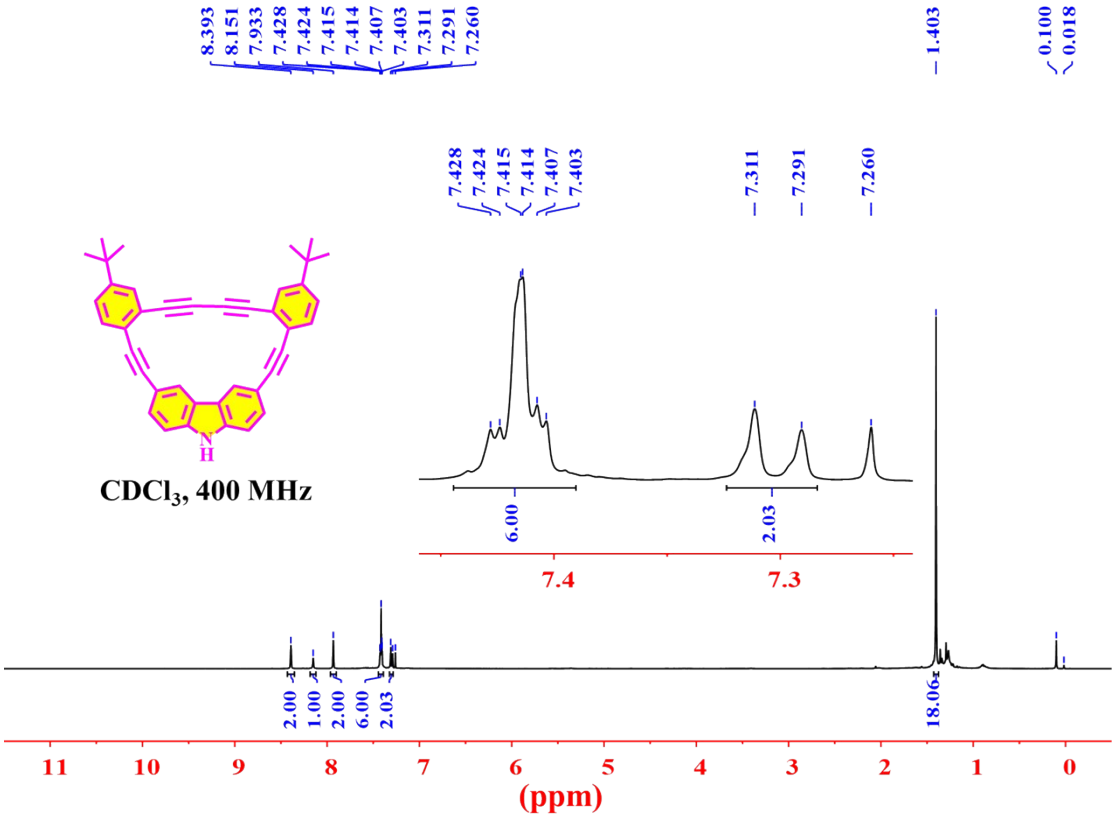

Fig. S13 ^{1}H NMR spectrum of compound **azaDBAa**.

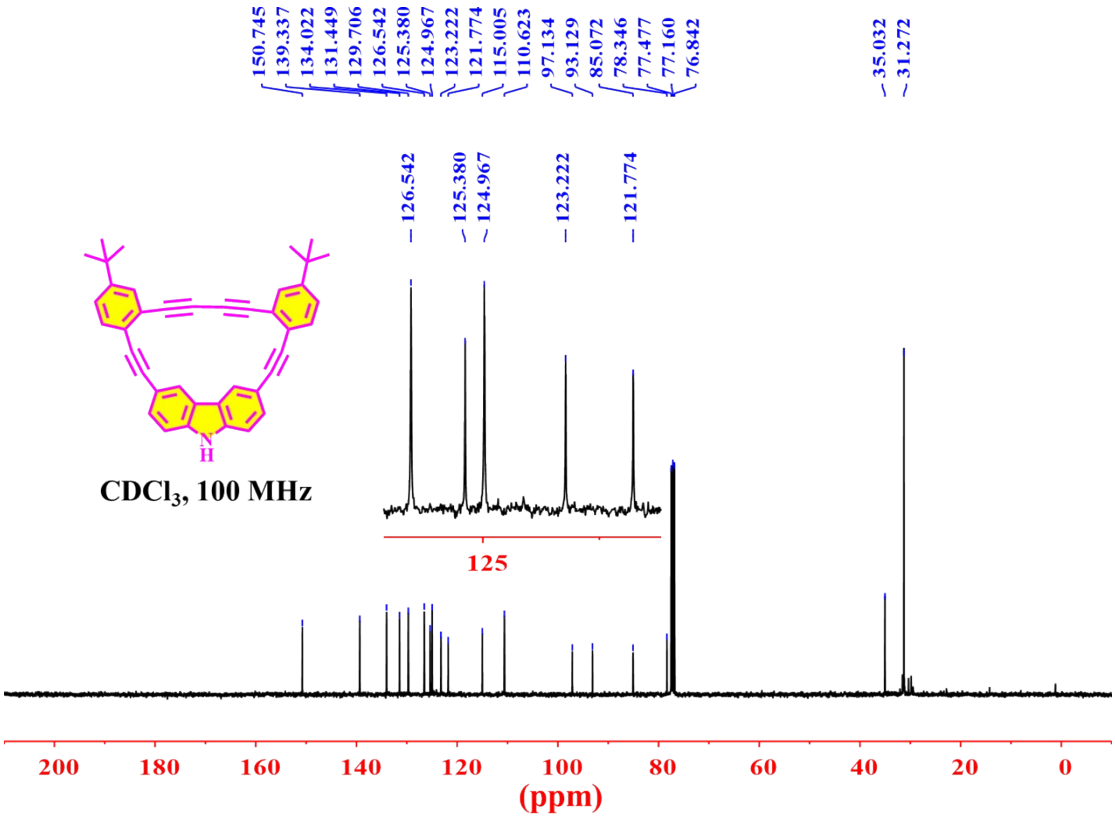

Fig. S14 ^{13}C NMR spectrum of compound **azaDBAa**.

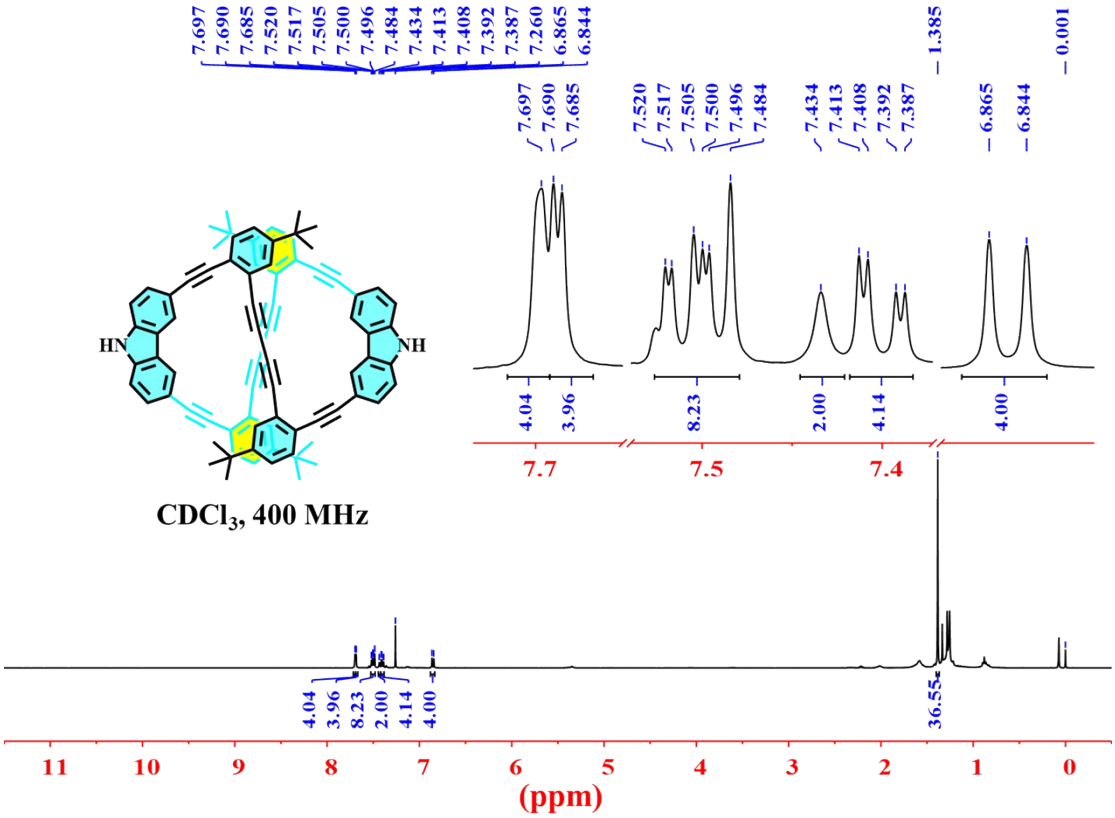

Fig. S15 ^{1}H NMR spectrum of compound **azaDBAb**.

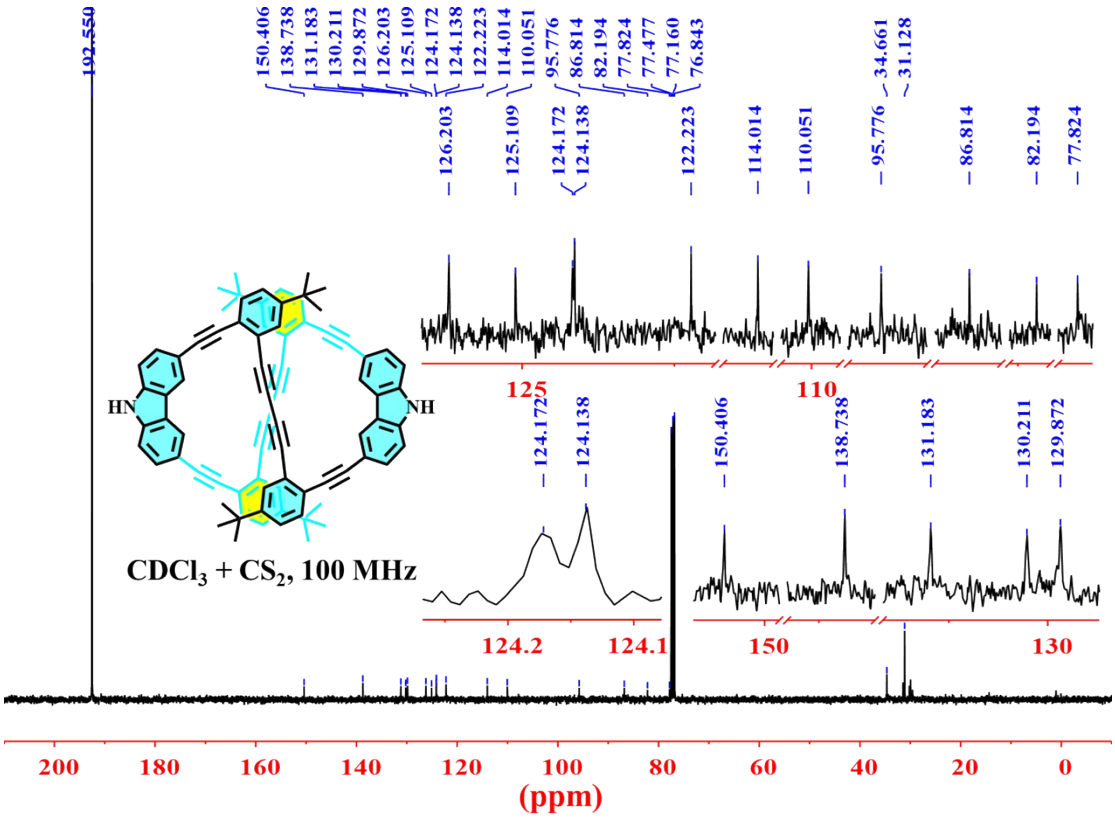

Fig. S16 ^{13}C NMR spectrum of compound **azaDBAb**.

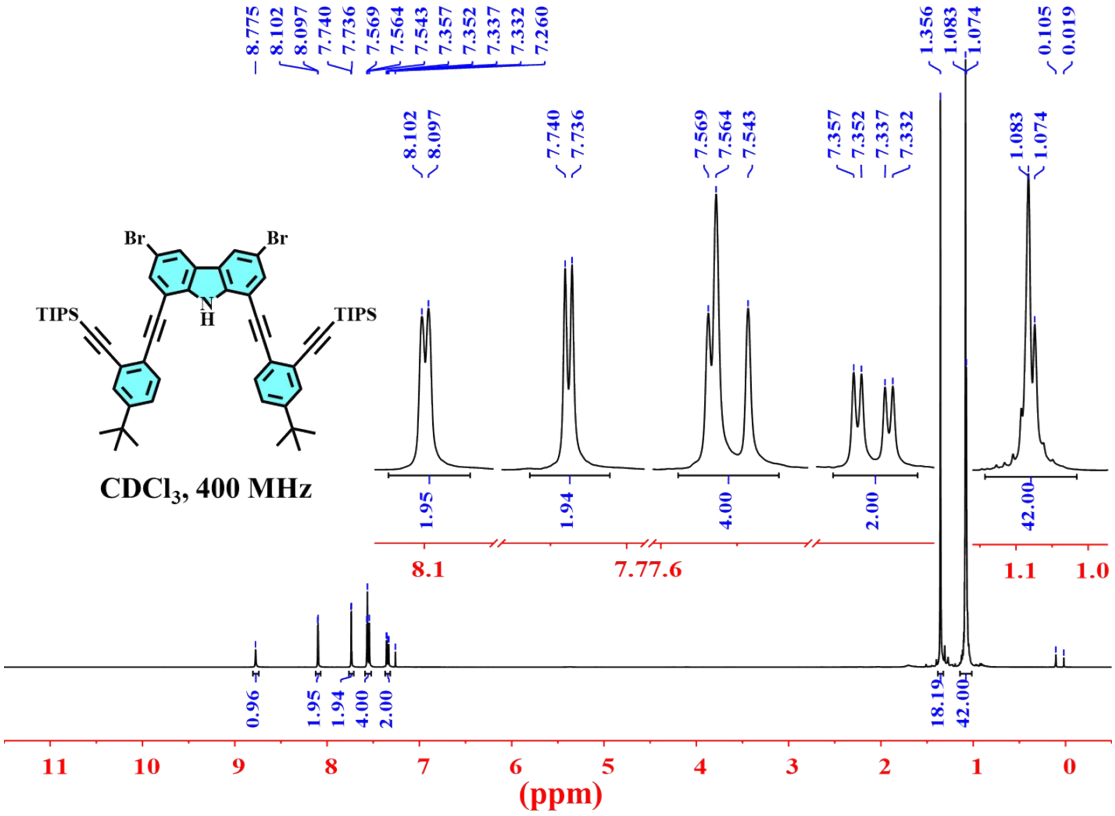

Fig. S17 ^{1}H NMR spectrum of compound **9**.

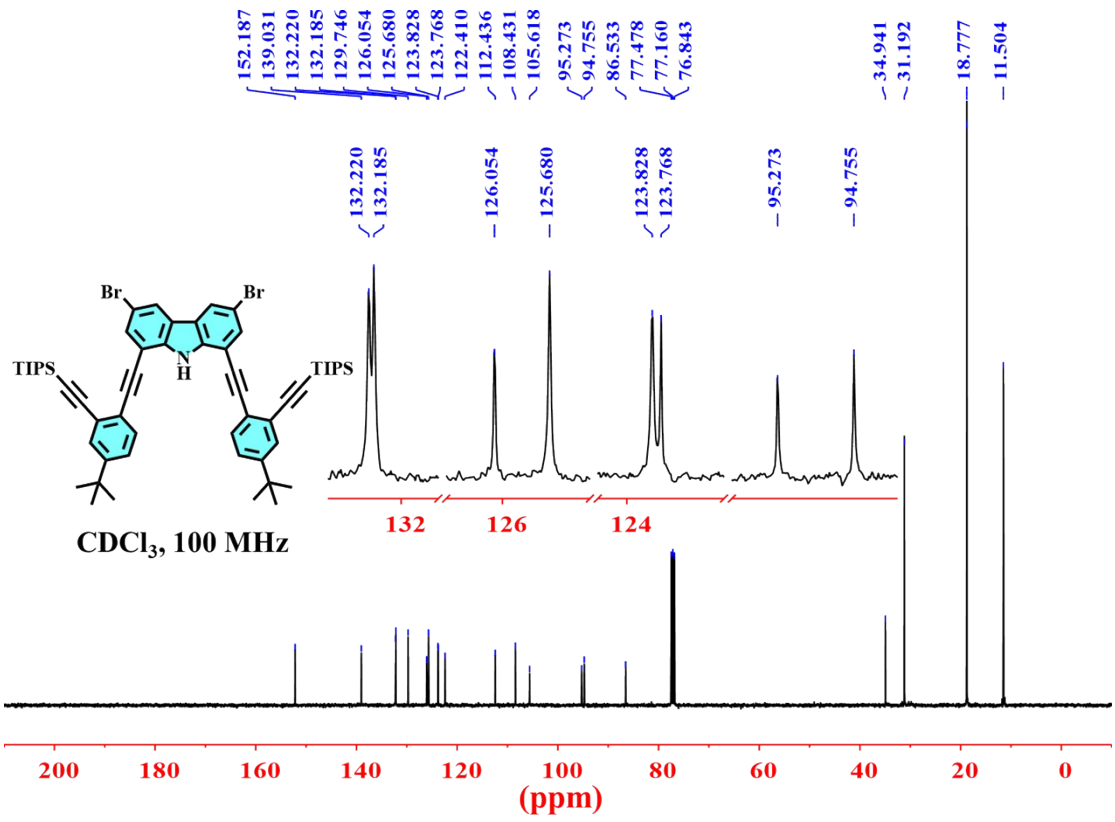

Fig. S18 ^{13}C NMR spectrum of compound **9**.

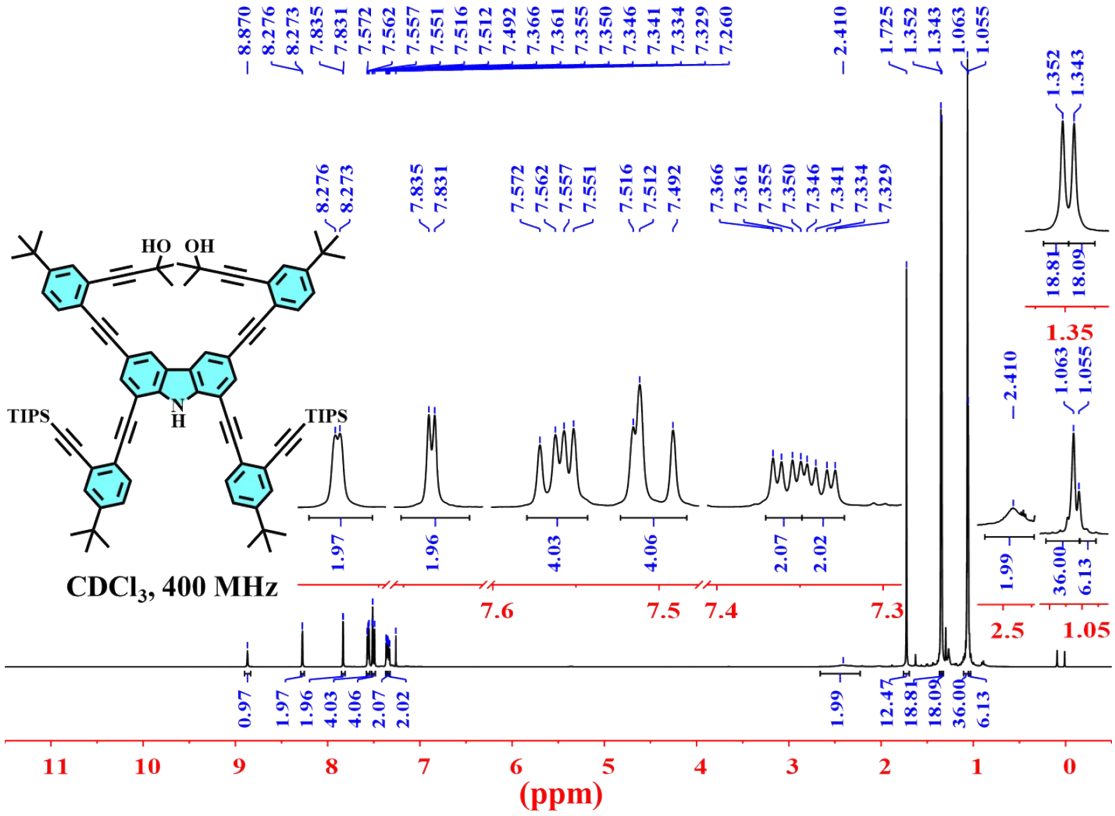

Fig. S19 ^{1}H NMR spectrum of compound **10**.

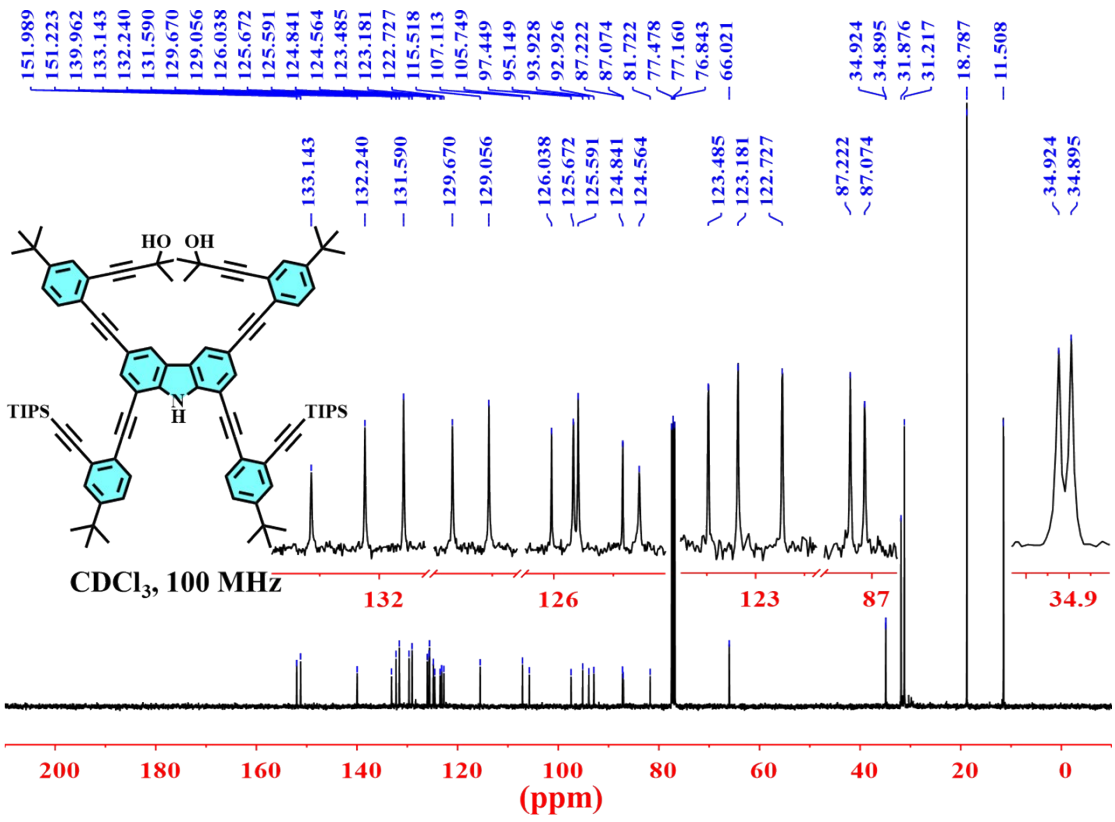

Fig. S20 ^{13}C NMR spectrum of compound **10**.

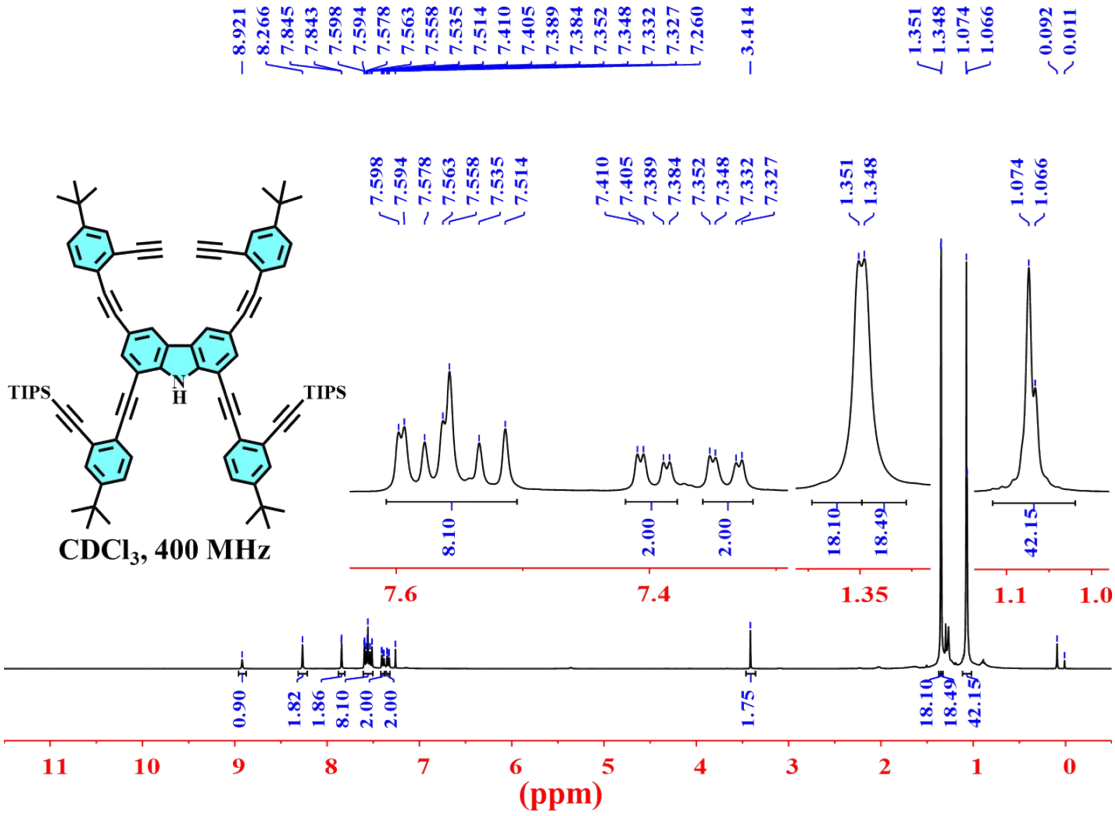

Fig. S21 ^{1}H NMR spectrum of compound **11**.

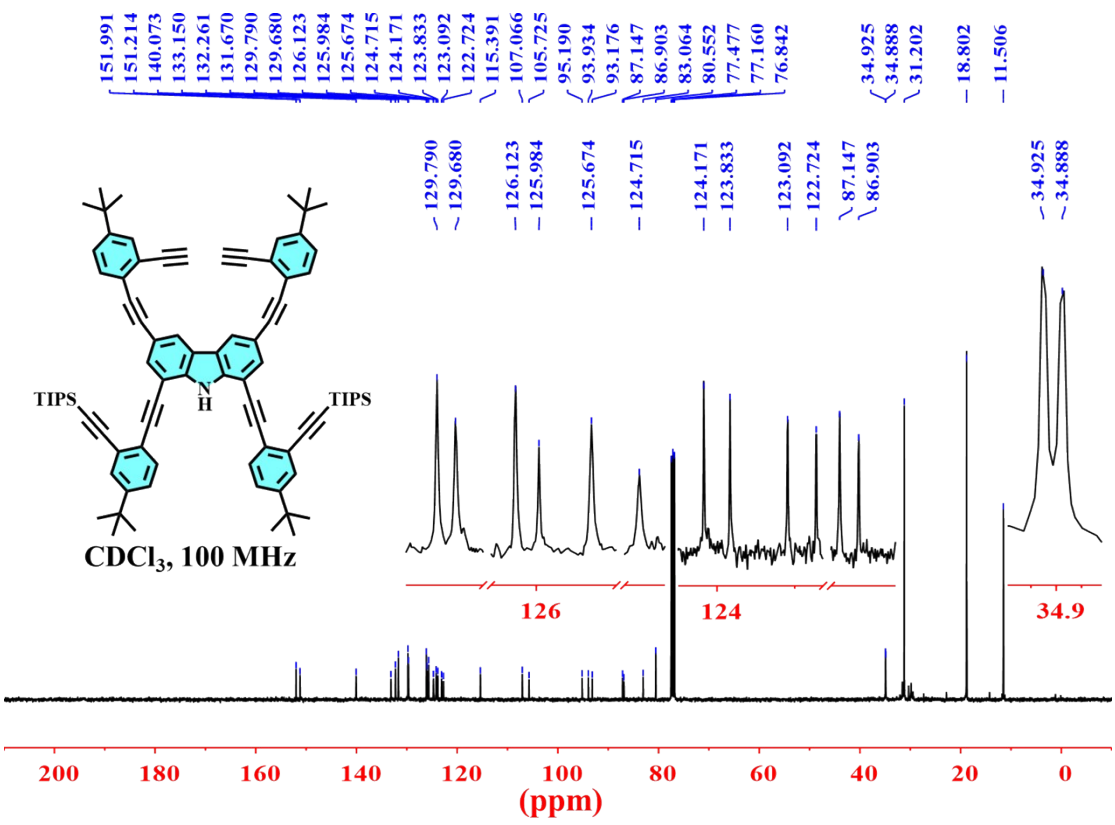

Fig. S22 ^{13}C NMR spectrum of compound **11**.

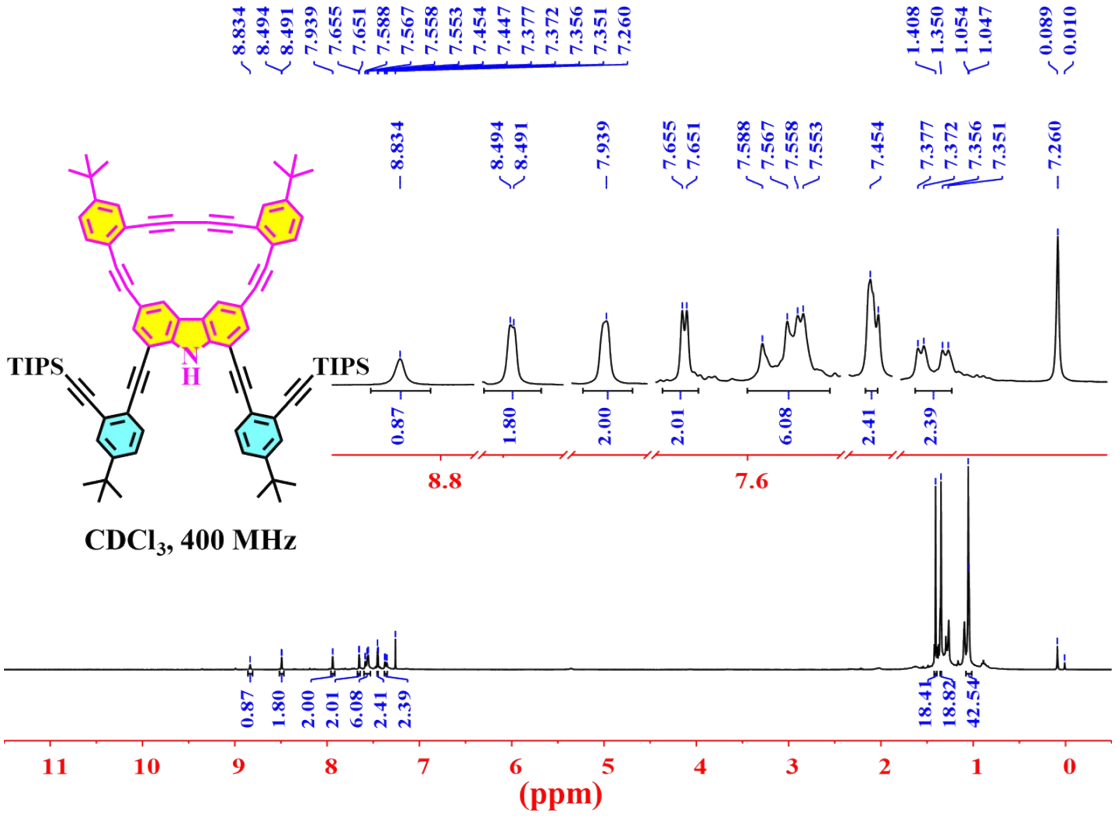

Fig. S23 ^{1}H NMR spectrum of compound **azaDBAc**.

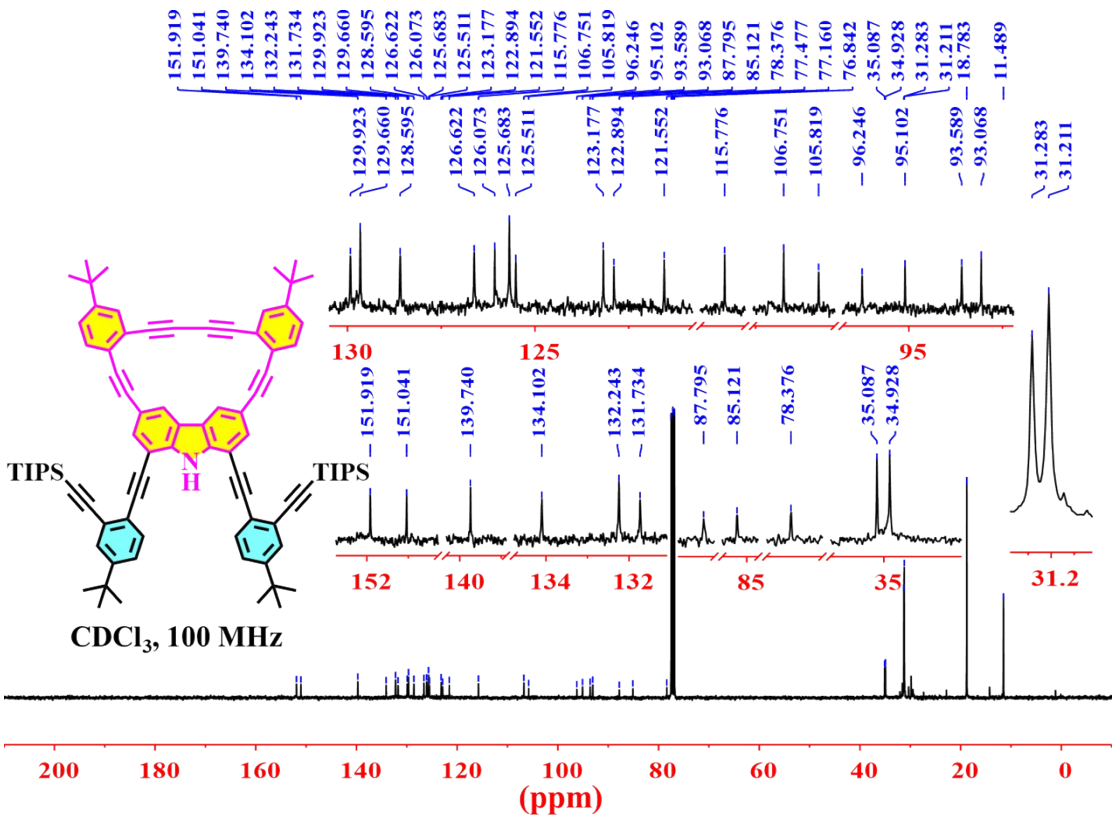

Fig. S24 ^{13}C NMR spectrum of compound **azaDBAc**.

5. Structural analysis for azaDBAs

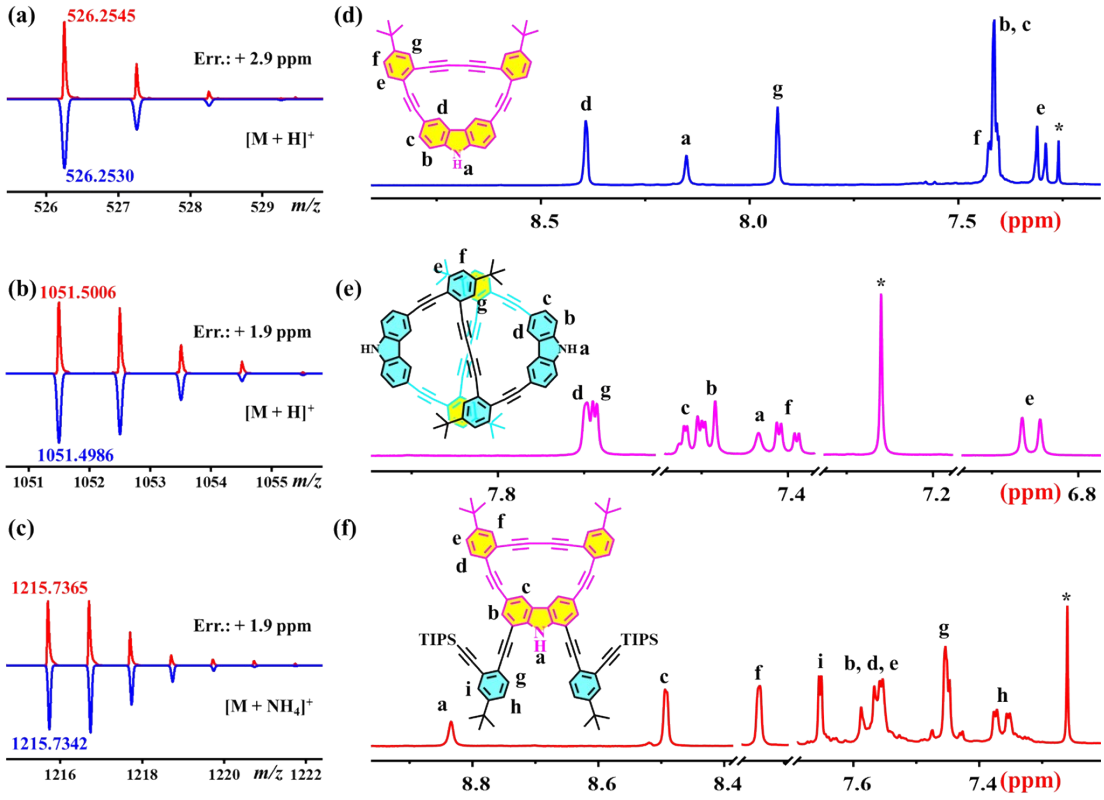

Fig. S25 Comparisons of measured (red lines) HR-MS and simulated (blue lines) isotopic distribution patterns of **azaDBAa** (ESI) (a), **azaDBAb** (APCI) (b), and **azaDBAc** (ESI) (c). Partial ^{1}H NMR spectrum in $CDCl_3$ at room temperature of **azaDBAa** (d), **azaDBAb** (e), and **azaDBAc** (f), and possible peak assignments of protons on the aromatic rings. The peaks labeled with asterisk arise from the residue peaks in the deuterium solvents.

As shown in Fig. S25a–c, the isotopic mass peak pattern of quasi-molecular ions $[M + H]^+$ (**azaDBAa** and **azaDBAb**) and $[M + NH_4]^+$ (**azaDBAc**) obtained by HR-ESI-Orbitrap-MS (**azaDBAa** and **azaDBAc**) and HR-APCI-Orbitrap-MS (**azaDBAb**) were in good agreement with their simulated values. Furthermore, based on the structural data, including chemical shifts and coupling constants, and referring to our previous reports[S1] along with a comparison of the ^{1}H NMR spectra with the corresponding cyclization precursors, possible peak assignments of protons on the aromatic rings of **azaDBAs** were proposed (Fig. S25d–f).

Generally, due to the anisotropic shielding effect of the ring current,[S2] the signals of

intra-annular protons of the annulene ring often appear in a relatively upfield region (*e.g.*, porphyrins[S3] and [18]annulene[S4]). However, compared to the corresponding proton signal in precursor **6** (8.28 ppm, Fig. S11), the proton *d* signal of **azaDBAa** did not exhibit a significant shift (8.39 ppm, Fig. S13). On one hand, the ring current generated by the [18]annulene produced a through-space shielding effect inside the ring. On the other hand, compared to precursor **6**, the rigid structure ring forced intra-annular proton *d* in **azaDBAa** to be inside the deshielding regions of those four alkynyl groups. Therefore, the above observation can be attributed to the combined effect of these two opposing anisotropic effects. In contrast, compared to the corresponding proton signals in precursor **6** and **azaDBAa**, the proton *d* signal in **azaDBAb** showed a significant upfield shift, observed at 7.70 ppm (Fig. S15). This phenomenon was mainly caused by the enlarged annulene ring size and weakened structural rigidity of **azaDBAb**, which prevented proton *b* from approaching the deshielding regions of the alkynyl groups as closely as in **azaDBAa**. Consequently, the anisotropic shielding effect from the annulene ring current in **azaDBAb** dominated over the deshielding effect of the alkynyl groups, causing the proton *b* signal to shift upfield. Compared to the proton *d* signal in **azaDBAa** (8.39 ppm), the corresponding proton *c* signal in **azaDBAc** was observed at 8.49 ppm (Fig. S23), showing a slight downfield shift. This observation could be attributed to the electron-withdrawing effect of the two additional *o*-phenylene diethynyl substituents, which reduced the electron-donating ability of the carbazole group to the annulene ring. As a result, **azaDBAc** exhibited lower electron density in the annulene ring and a weaker ring current, thereby suppressing the through-space shielding effect of the annulene ring. The aforementioned structural data and analysis demonstrated the synthesis of **azaDBAs** were successfully achieved.

6. Additional photophysical data

Table S1. Electronic Absorption and Emission Data for **azaDBAs**[a]

Solvent	Compd	λ_{abs} (nm) (ε (M^{-1} cm^{-1}))[b]	λ_{em} (nm)[c] (τ (ns))[d]	Φ_F (%)[e]
THF	**azaDBAa**	309 (34100)	443 (0.2, 1.6)	26.8
	azaDBAb	303 (74900)	456 (0.4, 1.3)	16.4
	azaDBAc	318 (42500)	434 (0.6, 2.7)	30.7
ACN	**azaDBAa**	307 (51300)	463 (1.7, 0.1)	34.4
	azaDBAb	301 (85200)	475 (4.1)	19.6
	azaDBAc	316 (44200)	453 (0.4, 2.4)	36.3
DMF	**azaDBAa**	310 (44900)	471 (5.6)	33.3
	azaDBAb	303 (71100)	492 (6.0)	16.0
	azaDBAc	318 (55300)	463 (0.3, 4.5)	34.2
EA	**azaDBAa**	308 (61900)	441 (0.2, 1.3)	26.7
	azaDBAb	301 (79800)	452 (0.2, 1.2)	20.4
	azaDBAc	317 (45600)	430 (0.3, 0.8)	28.2

[a]All Data were obtained at 298 K. [b]$c = 1 \times 10^{-5}$ M. [c]$c = 1 \times 10^{-6}$ M, $\lambda_{ex} = 320$ nm. [d]$c = 1 \times 10^{-6}$ M, $\lambda_{ex} = 403$ nm. [e]Relative luminescence quantum yield using quinine sulfate as the reference ($\Phi_F = 52\%$ in 0.05 M sulfuric acid aqueous solution).

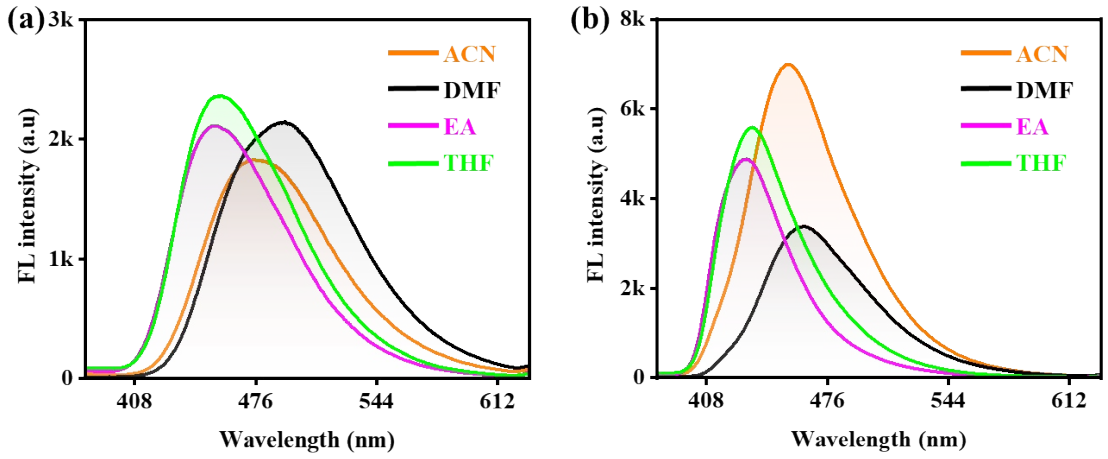

Fig. S26 Solvent-dependent fluorescence spectra of **azaDBAb** (b), and **azaDBAc** (c) at 298 K ($c = 1.0 \times 10^{-6}$ M, $\lambda_{ex} = 320$ nm).

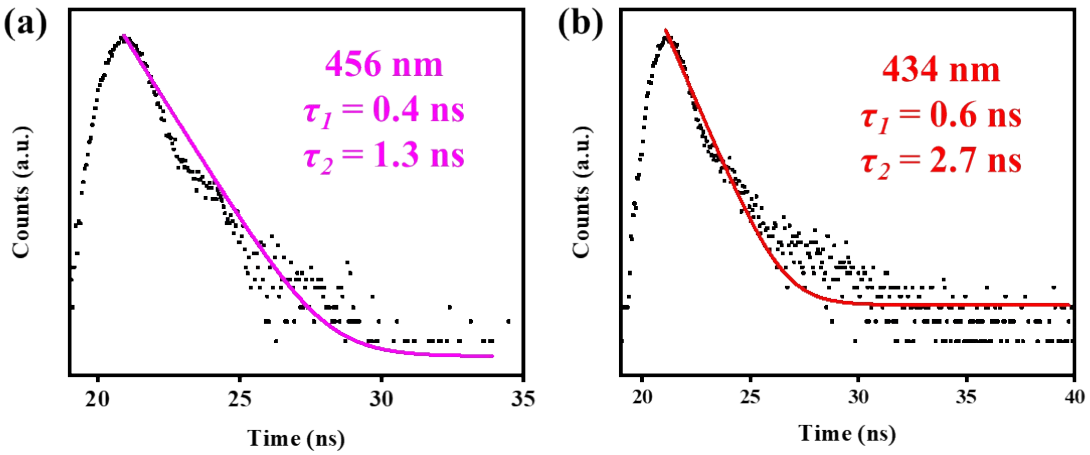

Fig. S27 Luminescent decay time (τ) and profile of **azaDBAb** (b), and **azaDBAc** (c) with the solid lines as the fitting curves. All measurements were performed in THF with a concentration of 1×10^{-6} M at 298 K, using a nanosecond pulsed laser system.

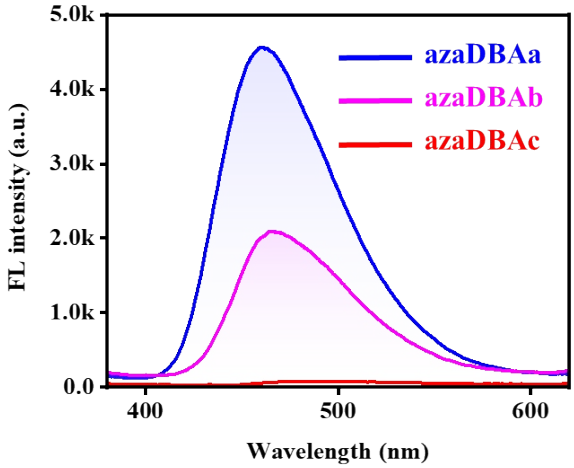

Fig. S28 Fluorescence spectra (λ_{ex} 320 nm) of **azaDBAs** in solid state.

Fluorescence emission of **azaDBAs** was observed in the range of 405–605 nm in the solid state, maximized at 460, 464, and 484 nm for **azaDBAa**, **azaDBAb**, and **azaDBAc**, respectively (Fig. S28). Compared with their corresponding fluorescence spectra in the solid state, the ECL emission showed a significant red shift, which may be attributed to the formation of different excimers under the excitation process of electrochemistry.

7. Measurement of the ECL signals of azaDBAs

Dissolve **azaDBAa**, **azaDBAb**, and **azaDBAc** powder (each at 1.0×10^{-6} mol) separately in 1 mL of tetrahydrofuran to prepare **azaDBAa**, **azaDBAb**, and **azaDBAc** solutions at a concentration of 1.0×10^{-3} mol/L. Subsequently, each of the solutions was dispensed in 10 μL aliquots onto a glassy carbon electrode (GCE, Φ = 4 mm) and air-dried at room temperature, yielding **azaDBAa**-, **azaDBAb**-, and **azaDBAc**-modified GCEs. The above-mentioned GCEs were individually immersed in 0.1 M phosphate-buffered solution (PBS, pH 7.4) containing 9.5 mM $S_2O_8^{2-}$, and the ECL signals of **azaDBAa**, **azaDBAb**, and **azaDBAc** were measured using an MPI-A ECL analyzer (Xi'an Remax Electronic Science & Technology Co. Ltd., Xi'an, China). A classic three-electrode system was adopted, the modified GCE was used as the working electrode, the platinum wire was used as the counter electrode, and the Ag/AgCl was used as the reference electrode. The photomultiplier tube voltage was biased at 800 V, the scanning potential was 0 V to −2 V, and the scan rate was 0.3 V/s.

Measurement of the ECL spectra of azaDBAs

The ECL emission spectra of **azaDBAs** were recorded on an RPSE-A spectroscopy detector (Xi'an Remax Electronic Science & Technology Co.Ltd., Xi'an, China) within a conventional three-electrode system (a modified GCE as the working electrode, Ag/AgCl as the reference electrode, and a Pt wire as the counter electrode). Specifically, **azaDBAa**, **azaDBAb**, and **azaDBAc** powders were dissolved separately in tetrahydrofuran to prepare 1.0×10^{-3} mol/L solutions of **azaDBAa**, **azaDBAb**, and **azaDBAc**. Subsequently, each solution was dispensed in 10 μL aliquots onto GCE and air-dried at room temperature to obtain **azaDBAa**-, **azaDBAb**-, and **azaDBAc**-modified GCE. The **azaDBAa**-, **azaDBAb**-, and **azaDBAc**-modified GCEs were individually measured in a 2 mL PBS (0.1 M, pH 7.4) solution containing 9.5 mM $S_2O_8^{2-}$ to get their ECL spectra. The instrumental parameters were set as follows: a sampling interval of 500 ms, a sensitivity of 1×10^{-3}, and a potential scan rate of 0.05 V/s.

ECL analysis of the sensor for EP

The **azaDBAc**-modified was dipped into 2 mL of PBS containing 9.5 mM $S_2O_8^{2-}$

and different concentrations of EP for the analysis of EP. The photomultiplier tube was configured with a voltage of 800 V, and the potential range was set from 0 to −2 V.

8. Notes and references

[S1] (a) P. Xu, N. Sun, X. Cao, H. Xie, Y. Zuo, H. Jia, J. Ding, Q. Huang, and J. Zhang, Curved π-conjugated dehydrobenzoannulene as an electron acceptor enabling fluorescence and electrochemiluminescence emission, *Org. Lett.,* 2025, **27**, 2868–2872; (b) P. Xu, N. Sun, H. Xie, Y. Zuo, X. Cao, H. Jia, Q. Huang, J. Ding, and J. Zhang, Luminescent carbazole-based electron donor–acceptor rings: synthesis, structure, and application, *Org. Chem. Front.,* 2025, **12**, 3462–3468.

[S2] (a) B. Hou, K. Li, H. He, J. Hu, Z. Xu, Q. Xiang, P. Wang, X. Chen, and Z. Sun, Stable crystalline nanohoop radical and its self-association promoted by van der Waals interactions, *Angew. Chem. Int. Ed.,* 2023, **62**, e202301046; (b) S. Wang, M. Tang, L. Wu, L. Bian, L. Jiang, J. Liu, Z.-B. Tang, Y. Liang, and Z. Liu, Linear nonalternant isomers of acenes fusing multiple azulene units, *Angew. Chem. Int. Ed.,* 2022, **61**, e202205658; (c) Y. Fan, J. He, L. Liu, G. Liu, S. Guo, Z. Lian, X. Li, W. Guo, X. Chen, Y. Wang, and H. Jiang, Chiral carbon nanorings: synthesis, properties and hierarchical self-assembly of chiral ternary complexes featuring a narcissistic chiral self-recognition for chiral amines, *Angew. Chem. Int. Ed.,* 2023, **62**, e202304623.

[S3] N. Abuhafez, A. W. Ehlers, B. de Bruin, and R. Gramage-Doria, Markovnikov-selective cobalt-catalyzed wacker-type oxidation of styrenes into ketones under ambient conditions enabled by hydrogen bonding, *Angew. Chem. Int. Ed.,* 2024, **63**, e202316825.

[S4] W. Stawski, Y. Zhu, I. Rončević, Z. Wei, M. A. Petrukhina, and H. L. Anderson, The anti-aromatic dianion and aromatic tetraanion of [18]annulene, *Nat. Chem.,* 2024, **16**, 998–1002.